

Effect of Manufacturing Tolerance to the Thrust Characteristics of the Cylindrical Switched Reluctance Linear Synchronous Motor (SRLSM)

Fairul Azhar^{1,2,*}, Hiroyuki Wakiwaka³, and Kunihisa Tashiro³

¹Faculty of Electrical Technology and Engineering
Universiti Teknikal Malaysia Melaka (UTeM), Hang Tuah Jaya, Durian Tunggal, 76100 Melaka, Malaysia

²Electrical Machine Design, EV Pro Drives Research Group

CeRIA, UTeM, Hang Tuah Jaya, Durian Tunggal, 76100 Melaka, Malaysia

³Faculty of Engineering, Shinshu University, 4-17-1 Wakasato, Nagano 380-8553, Japan

ABSTRACT: Manufacturing tolerances introduce unavoidable dimensional deviations in electrical machine components. In the case of switched reluctance linear synchronous motors (SRLSMs), the manufacturing tolerance, Δx , may significantly affect the thrust characteristics. Therefore, a systematic investigation of the impact of manufacturing tolerance, Δx , on the thrust characteristics of a cylindrical SRLSM through finite element analysis and experimental validation is presented. Two mover shafts with different tolerance control strategies, denoted as S45C-01 and S45C-02, were fabricated. Based on the findings, accumulated tolerances of $-562.3 \mu\text{m}$ and $-20 \mu\text{m}$ for S45C-01 and S45C-02, respectively, were acquired using a vision measuring system. Then, a model that incorporated the accumulated manufacturing tolerance, Δx , was created and simulated. Thrust characteristics were evaluated under both ideal and tolerance inclusive conditions and experimentally measured over a current range of 0.1–1.0 A. The results indicate that neglecting manufacturing tolerance leads to substantial discrepancies between the simulated and measured thrusts, particularly at low excitation currents, with thrust errors exceeding 200%. When the measured manufacturing tolerances were included in the simulation, the thrust error was significantly reduced to below 8.4% for S45C-01 and below 4% for S45C-02, demonstrating close agreement with the experimental results. The findings confirm that manufacturing tolerance is a critical factor in accurately predicting SRLSM thrust performance and that tolerance-inclusive modeling substantially improves the reliability of simulation-based performance evaluation.

1. INTRODUCTION

Switched reluctance linear synchronous motor (SRLSM) is a type of synchronous machine. It can produce linear motion in the absence of a motion translator. Generally, an SRLSM consists of two parts: the stator and the mover. The primary performance metric of the SRLM is its thrust. Thrust is defined as the ability to move loads with precision and speed. Furthermore, constant and flat thrust is required for numerous applications despite the main drawbacks of the SRLSM, which are its relatively high thrust ripple and acoustic noise [1, 2]. During the structural design stage of the SRLSM, structural optimization involves the arrangement and geometry of the stator and mover poles, phase configuration, and material, which are often used to increase thrust [3–6]. During the operation of the SRLSM, a driving system with advanced control strategies is used to improve the thrust profile and provide smooth operation of the SRLSM [7, 8].

The main drawbacks of the SRLSM are its thrust ripple, which increases the acoustic noise and vibration effect [9–12]. Factors that contribute to the existence of thrust ripples in SRLSM include double salient structure [13], nonlinear region

operation that leads to a nonlinear inductance profile [13, 14], and nonuniform and varying structural dimensions. Nonuniform and varying structural dimensions can be caused by manufacturing tolerance [1, 2, 15]. In the case of electrical machine construction, manufacturing tolerances refer to the permissible limits of variation in the physical dimensions and material properties during production, such as air-gap width, magnet placement, winding spacing, and back iron thickness. These tolerances are inherent to any manufacturing process and directly influence the electromagnetic and mechanical performance [1, 16, 17].

Manufacturing tolerances can cause minor deviations in the SRLSM dimensions. However, minor deviations in key dimensions, such as air gaps, winding spacing, and tooth dimensions, can significantly affect the thrust performance of the SRLSM [2]. At the air gap, the manufacturing tolerance can cause an increment in the air gap length compared to the original design. Furthermore, it could introduce eccentricity issues. On the teeth side, the combination of multiple manufacturing tolerances on adjacent teeth may cause the position of the teeth on the mover and stator sides to vary. For example, positions where all teeth on both sides are supposedly in a fully aligned position, but some tooth pairs may shift into partially aligned positions. This condition led to an uneven electromag-

* Corresponding author: Fairul Azhar bin Abdul Shukor (fairul.azhar@utem.edu.my).

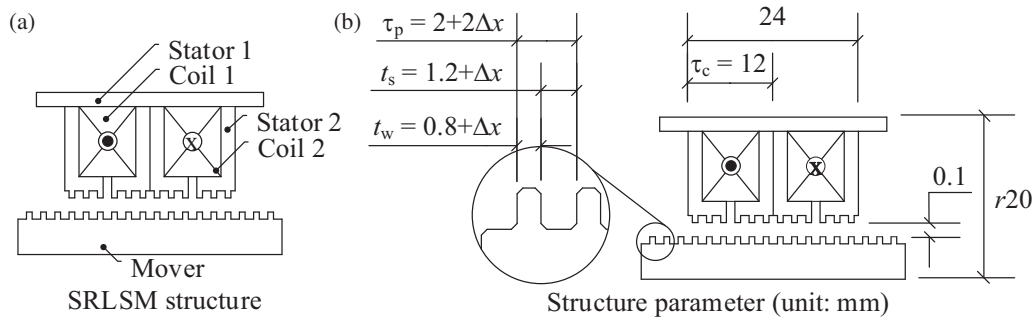


FIGURE 1. SRLSM structure with consideration of the manufacturing tolerance, Δx .

TABLE 1. Detailed design structure and operating parameters of the SRLSM.

Category	Parameters	Value
Structure parameters	Total outer radius, r_{total} (mm)	20
	Coil pitch, τ_c (mm)	12
	Teeth pitch, τ_p (mm)	2
	Slot width, t_s (mm)	1.2
	Teeth width, t_w (mm)	0.8
	Teeth depth, t_d (mm)	1
	Mover radius, r_s (mm)	6
	Air gap length, δ (mm)	0.1
Electrical parameters	Coil resistance (per coil), R (Ω)	6.5
	Coil turn (per coil), N	336
	Copper wire diameter, ϕ_C (mm)	0.32
	Supply current, I (A)	0.1–1.0 A
Thrust characteristics measurement range	Displacement cycle (mm)	2.0
	Displacement resolution (mm)	0.1

netic force distribution and increased further thrust ripple [18]. Therefore, in this study, the effect of manufacturing tolerance on the thrust characteristics of the SRLSM is investigated.

2. BASIC PRINCIPLE OF THE SRLSM

The SRLSM model is shown in Fig. 1. It has two-coil winds on the stator yoke to construct the stator part. Meanwhile, a cylinder-shaped tooth iron is used as the mover. The coil pitch, τ_c , of the SRLSM was set to 12 mm and the tooth pitch for the stator and mover set to 2 mm. The teeth pitch, τ_p , has been divided into two parts: slot width, t_s , and tooth width, t_w , which have dimensions of 0.8 mm and 1.2 mm, respectively.

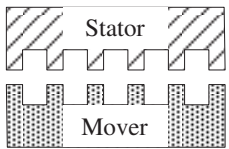
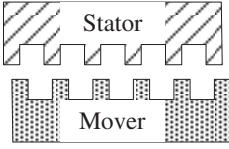
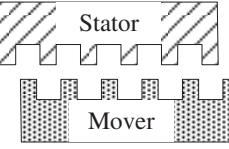
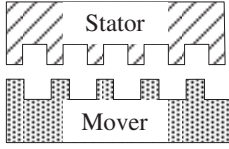
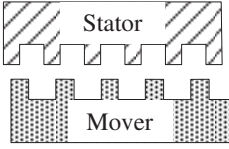
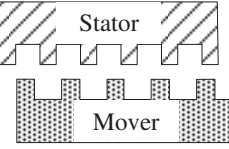
The SRLSM was designed and fabricated in a cylindrical shape. Therefore, the manufacturing tolerance is only considered for the dimensions of the teeth of the mover part. To minimize the other manufacturing effect, each edge of the SRLSM was created based on a fillet edge with a radius of 0.1 mm. The outer side of the stator yoke was extended in the manufactured prototype to place the bearing. The detailed designed structure and operating parameters of the SRLSM are listed in Table 1.

The thrust in the SRLSM is produced as the mover approaches and reaches full magnetic alignment with the stator, where the magnetic reluctance is minimized. The value is in-

fluenced by the position of the mover and stator teeth. There are three categories of positions: (i) fully aligned, (ii) partially aligned, and (iii) fully unaligned. The fully aligned position is defined as the position at which all the mover and stator teeth are directly opposite each other. In this position, the thrust is 0 N, and the magnetic reluctance is minimum [18, 19]. However, the fully unaligned position is defined as the position of the teeth of the mover in the center of the stator slot. In this position, the thrust is still 0 N, but the magnetic reluctance is maximum [18, 19]. The position between these two positions is called partially aligned. The thrust of the SRLSM is developed during this type of position, where the mover has a tendency to move into either fully aligned or fully unaligned positions.

When no manufacturing tolerance is considered, the positions of all teeth will be the same according to one of the position conditions above. Therefore, the thrust distribution among all the teeth is balanced. However, when manufacturing tolerance occurs, the teeth are shifted due to the accumulated value of the manufacturing tolerance. This condition resulted in an unbalanced thrust distribution among the teeth and reduced the thrust compared to the case when no manufacturing tolerance was considered. The effect of manufacturing tolerance on the tooth position of the SRLSM is shown in Table 2.

TABLE 2. Position of the SRLSM.

	(a) Fully aligned	(b) Partially aligned	(c) Fully unaligned
Zero manufacturing tolerance			
Non-zero manufacturing tolerance			

The general expression for the SRLSM's thrust is as Equation (1). Based on Equation (1), the thrust of the SRLSM depends on its inductance profile.

$$F(x) = \frac{1}{2}i^2 \frac{dL(x)}{dx} \quad (1)$$

where $F(x)$ is the thrust in the function of mover displacement, x in (N); i is the current in (A); and $L(x)$ is the inductance in the function of mover displacement, x in (H).

The inductance is associated with permeance, P , as expressed in Equation (2).

$$L(x) = N^2 P(x) \quad (2)$$

where N is the winding turn, and $P(x)$ is the permeance in the function of mover displacement, x in (H).

The permeance, $P(x)$, is closely related to the structural parameters. In the SRLSM case, the structural parameters involve tooth dimension on both stator and mover parts, where the thrust is developed. The general expression for the permeance is shown in Equation (3).

$$P(x) = \frac{\mu_O(x)}{\delta} \quad (3)$$

where μ_O is the permeability of air with a value of $4\pi \times 10^{-7}$ H/m, and $A(x)$ and δ are the cross-sectional area of the permeance and the air-gap length in (m) and (m²), respectively.

The cross-sectional area of the permeance depends on the overlapping area between the stator and mover teeth. By considering manufacturing tolerances, Δx , the overlapping area will be inconsistent as shown in Table 2, hence reducing the area and thrust. The cross-sectional area in the function of manufacturing tolerance, Δx , is as in Equation (4). Therefore, the thrust equation now becomes Equation (5).

$$A(x, \Delta x) = (t_w(x) + \Delta x) \cdot (\pi r_{\text{total}}) \quad (4)$$

$$F(x) = \frac{1}{2}i^2 \frac{d}{dx} \left(\frac{N^2 \mu_O A(x, \Delta x)}{\delta} \right) \quad (5)$$

Manufacturing tolerance effects in electrical machines have been widely studied, particularly in permanent magnet and switched reluctance machines, where dimensional

variations can significantly influence electromagnetic performance [16, 17, 20]. Therefore, this paper aims to investigate the impact of accumulated manufacturing tolerance on thrust performance through both finite element method (FEM) and experimental approaches.

Table 3 presents a comparison between the present work and several recent studies addressing manufacturing tolerances in electric machines. It can be observed that previous works predominantly rely on statistical or simulation-based approaches, such as Monte Carlo methods, deep-learning-assisted robustness evaluation, and DOE-ANOVA-based sensitivity analysis [1, 21, 22]. While these studies provide valuable insights into tolerance-induced performance variations, they generally assume idealized or virtual tolerance distributions. In contrast, the present work emphasizes experimentally grounded tolerance effects, where the variations originate directly from fabricated components. Furthermore, unlike prior studies that focus on multi-phase systems and ripple-related metrics, this work specifically investigates the maximum thrust, F_{max} , performance of a single-phase structure, providing a more fundamental understanding of tolerance influence before extending to multi-phase configurations.

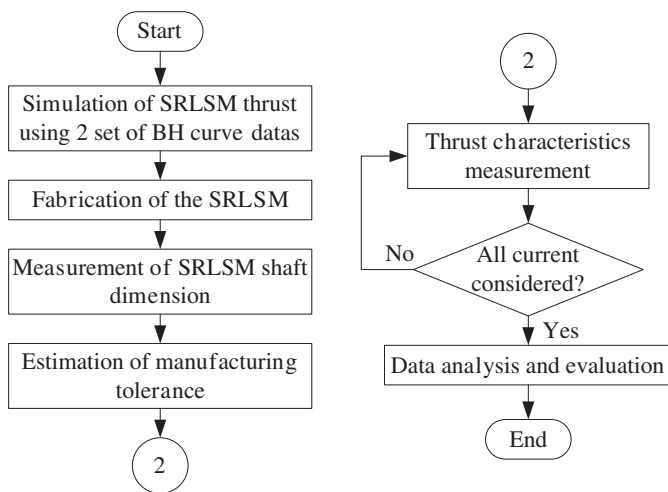
3. EVALUATION OF MANUFACTURING TOLERANCE'S EFFECT

In this section, the process of evaluating the effect of the manufacturing tolerance on the thrust of the SRLSM is discussed. The process started with the simulation of the SRLSM thrust using FEM software. To minimize the impact of variations in the **BH** curve data of the material used, two types of data were employed in the simulation. The first was the original data provided within the FEM software, and the second was the **BH** curve data measured based on the actual material used for fabrication. Subsequently, the SLRSM prototype was fabricated. For the stator, only one set of prototypes was fabricated, whereas for the mover shaft, two sets of prototypes were fabricated with different tolerance control mechanisms during the fabrication process. Both mover shafts undergo a dimension measuring process using a vision measuring system to accurately identify the manufacturing tolerances of every tooth of

TABLE 3. Comparison between the present work and several recent studies.

Aspect	Li et al. [1]	Nam et al. [21]	Ershad et al. [22]	This Work
Machine type	Ironless PM Linear Motor	CNC Servo Motor (PM motor)	PMSM Traction Motor	SR Linear Motor (Single-phase)
Primary Focus	Thrust ripple due to structural tolerances	Robust design with tolerance (DL-based)	Manufacturing variation effect on torque & energy loss	Manufacturing tolerance effect on thrust, F_{\max}
Analysis Method	Monte Carlo and FEA	DL surrogate, LHS and TOPSIS	DOE, ANOVA, and FEA	Simulation and experimental validation
Tolerance Treatment	Probabilistic	Statistical robustness metrics	Sensitivity contribution	Measured based on prototype
Considered Parameters	Magnet size, coil spacing, winding position	Multiple geometric design variables	Geometry, material and airgap variations	Geometric tolerances from fabrication
Experimental Validation	Not included (simulation-based)	Prototype built and tested	Correlation with experimental data	Prototype built and tested

the mover shaft. Then, the thrust of the SRLSM using both mover shafts was measured at a range of currents from 0.1 A to 1.0 A. The thrust results from the simulation and measurement were analyzed and compared to observe the effect of the manufacturing tolerance on the thrust. This process is illustrated in Fig. 2.

**FIGURE 2.** Process in determination of effect of the manufacturing tolerance, Δx , on the SRLSM thrust.

3.1. Thrust Simulation of the SRLSM

The SRLSM was simulated and fabricated using an S45C grade material. To reduce the effect of the variation in **BH** curve data on the thrust, two sets of data were used during the thrust simulation: (i) the default material data provided in the simulation software, and (ii) experimentally measured B-H characteristics obtained from the same grade of material used to fabricate the mover. Fig. 3(a) shows the differences between the **BH** curves. The curve shows a significant difference, especially at magnetic field strengths less than 10 kA/m. The FEM data provide a higher magnetic flux density than the measured **BH** curve,

particularly in this range. This discrepancy can lead to an over-estimation of the magnetic field density level in the simulation, resulting in predicted thrust values that are higher than the actual values. Consequently, the thrust characteristics may not be accurately estimated under low excitation conditions, where the material is far from saturation, and the nonlinear characteristics of the **BH** curve strongly influence force generation. However, for higher excitations, the difference was insignificant. These conditions are shown in Figs. 3(b) and (c), respectively. This step is done to isolate the influence of geometric tolerances on thrust performance and minimize the effect of magnetic property discrepancies, ensuring that the observed thrust variation is predominantly attributed to geometric tolerances.

3.2. Fabrication of the SRLSM Prototype

The SRLSM prototype was fabricated, as shown in Fig. 4(a). The SRLSM was placed vertically on a movable stage to vary the shaft mover displacement against its stator. At the bottom side of the shaft mover, a load cell was placed to read the thrust produced. Meanwhile, a 1 kg static load was placed on top of the shaft mover as a reference for the gravitational force, such that when no current was applied, the load cell could measure the combination of the static load and shaft mover weight. When current is injected into the motor, any additional force generated is reflected as a change in the load cell reading.

The shaft movers were fabricated using two different types of manufacturing tolerances. The shaft movers are labelled S45C-01 and S45C-02 and were fabricated with different lengths to ensure that they could be easily differentiated. The S45C-01 mover was manufactured with 18 teeth, while the S45C-02 was manufactured with 26 teeth. Fig. 4(b) shows the fabricated shafts of the SRLSM. During the measurement of the thrust characteristics, the two shaft movers were used sequentially, and outputs were analyzed and compared. The thrust characteristics were also measured over at least two cycles of the tooth pitch, τ_p , with a resolution of 0.1 mm so that a complete cycle of the thrust characteristics could be captured.

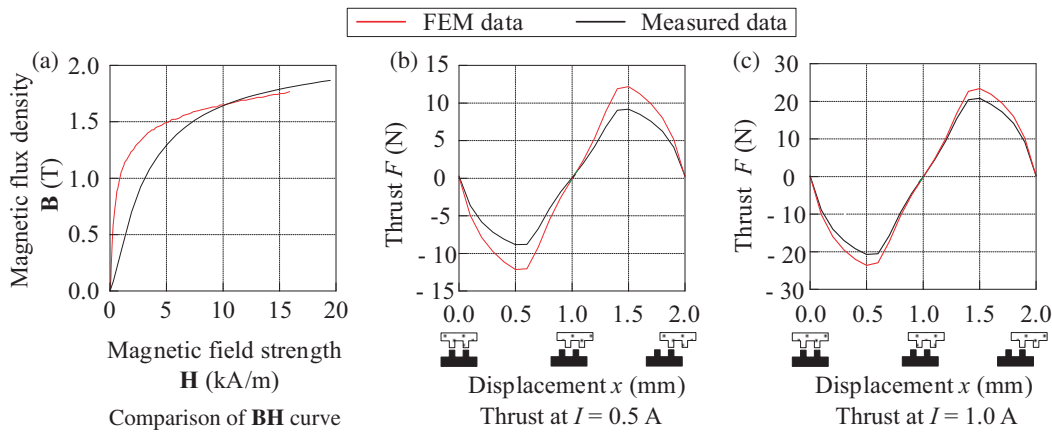


FIGURE 3. Comparison of BH curve data and thrust characteristics produce by it.

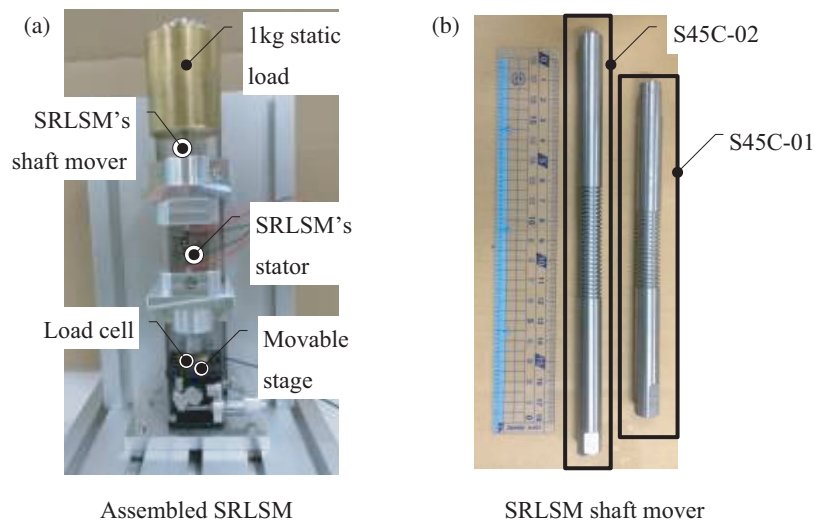


FIGURE 4. Manufactured SRLSM with two different shaft movers.

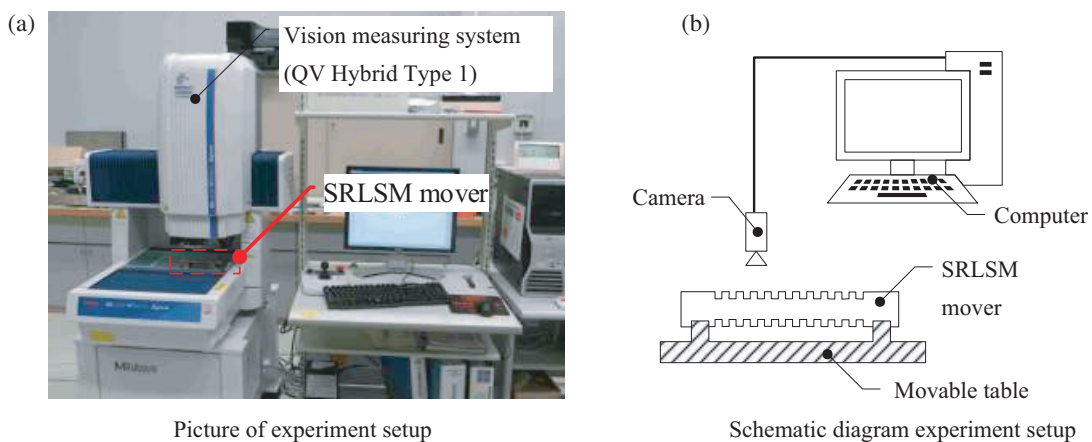


FIGURE 5. Experiment setup for the SRLSM's shaft mover dimension measurement.

3.3. Measurement of the Mover Shaft Manufacturing Tolerance

To check the manufacturing tolerance, Δx , the SRLSM shaft movers were measured using a vision measuring system, QV Hybrid Type 1 (QVH1 Apex 302 PRO3). This system can measure any specimen, such as the SRLSM shaft mover, up to four

decimal places in millimeters. Fig. 5 shows the experimental setup for the SRLSM measurements. The tooth components of the SRLSM mover were assigned identification numbers, as shown in Fig. 6. The tooth components, namely slot width, t_s , tooth width, t_w , and tooth pitch, τ_p , were measured and com-

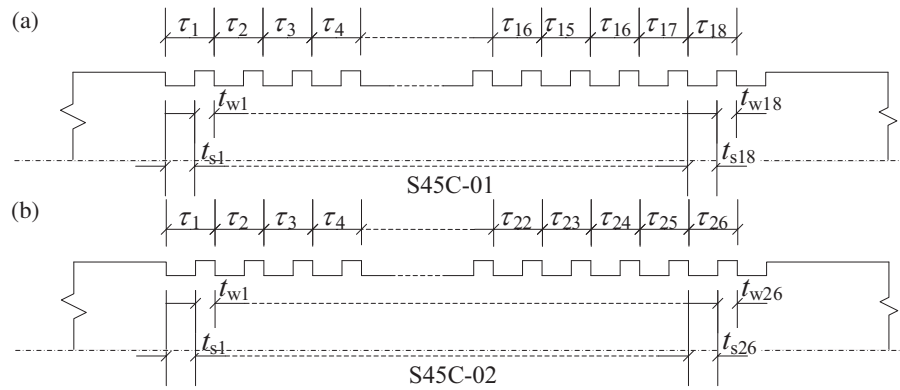


FIGURE 6. The SRLSM's mover teeth component identification number.

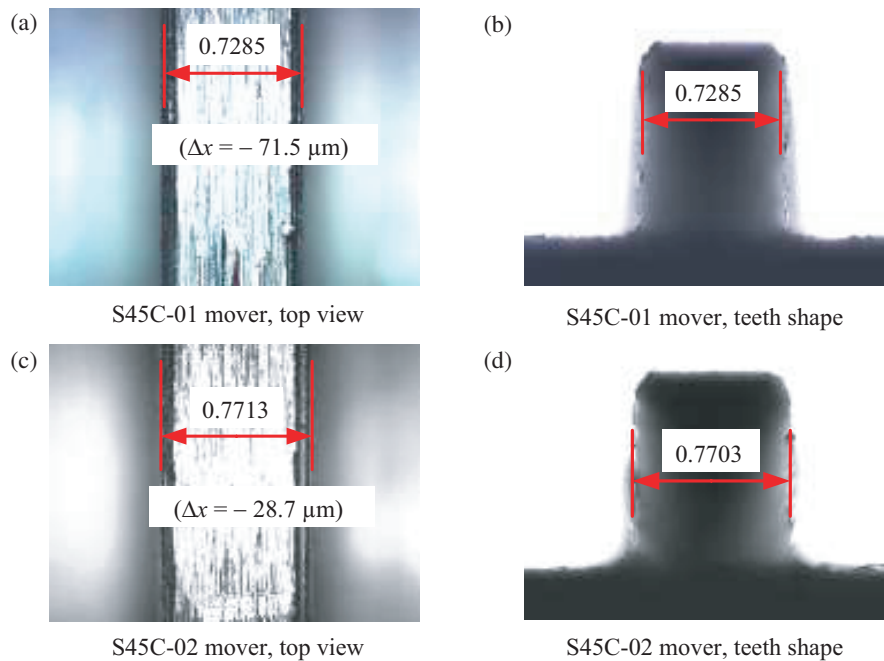


FIGURE 7. Sample of top view and teeth shape of the SRLSM's shaft mover.

pared with the design values. Fig. 7 shows a sample of the top view and tooth shape based on the vision system output during the SRLSM mover dimension measurement. For example, in Fig. 7(a), one of the teeth of the S45C-01 mover was fabricated with a thickness of 0.7285 mm compared to the design value of 0.8 mm. Therefore, the manufacturing tolerance for this tooth was $-71.5 \mu\text{m}$. The negative sign indicates that the teeth were fabricated smaller than the design values. The same pattern was found on the S45C-02 mover, where one of the teeth was fabricated smaller than its design value; hence, the resultant manufacturing tolerance was $-28.7 \mu\text{m}$. The manufacturing tolerances for all tooth parameters of both shafts were measured and recorded for the thrust characteristics' evaluation.

4. THRUST CHARACTERISTICS PERFORMANCE OF THE SRLSM

This section presents the results obtained from the analyses conducted in this study. The findings are organized into two main

sections: a comparison of the manufacturing tolerance between shaft movers and an evaluation of the thrust characteristics of the SRLSM under different shaft movers. These results provide insights into the relationship between manufacturing tolerance and thrust characteristics.

4.1. Comparison of Manufacturing Tolerance between Shaft Movers

During the shaft mover measurement process, the distances between adjacent edges were recorded to determine the actual length with a precision of $0.1 \mu\text{m}$. The base line for each distance was based on the design value as shown in Fig. 1. Fig. 8 depicts the measured dimensions of the mover teeth components for both shaft movers against their design values. It shows that for S45C-01, the deviation dimensions for the tooth width, t_w , slot width, t_s , and tooth pitch, τ_p , are almost consistent for each tooth. The tooth width, t_w , and tooth pitch, τ_p , were smaller than their design values, whereas the opposite condi-

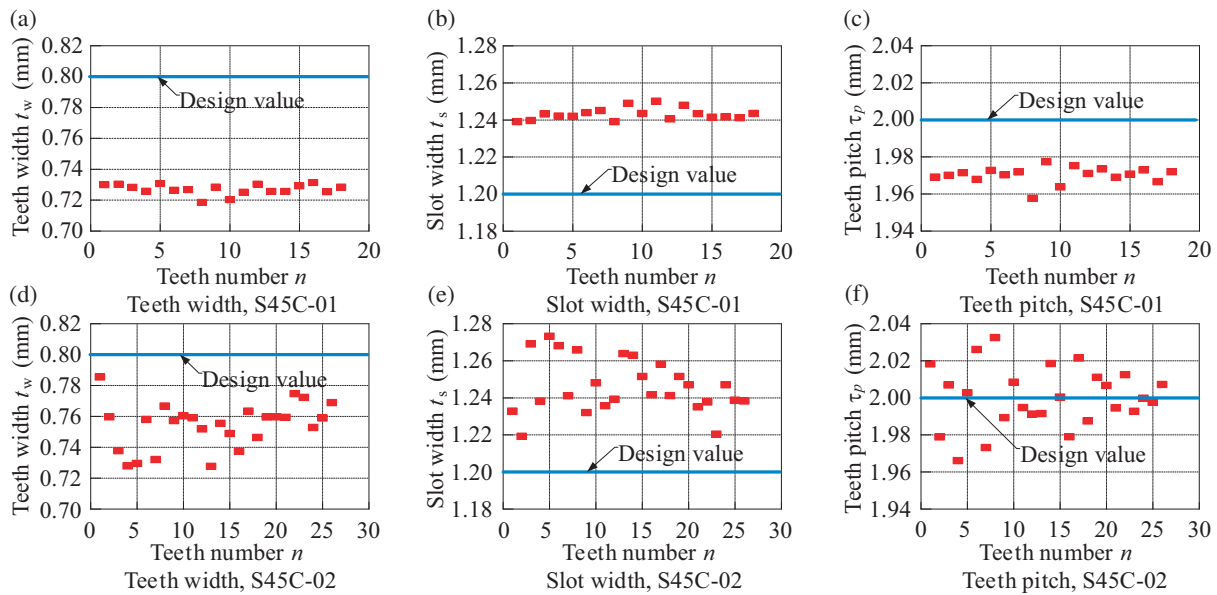


FIGURE 8. Shaft mover teeth component dimension.

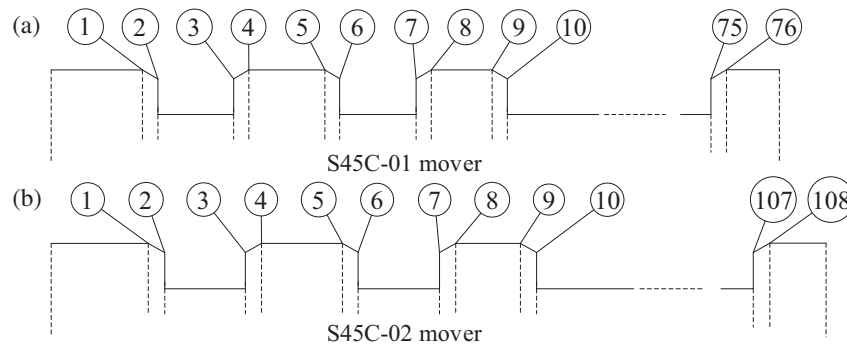


FIGURE 9. Measuring point of the SRLSM's movers, n_{mp} .

tion was observed for the slot width, t_s . The tooth width, t_w , was manufactured within the range of 0.72–0.73 mm, which is smaller than the designed value of 0.80 mm. Meanwhile, the tooth pitch, τ_p , ranged 1.96–1.98 mm, which is slightly lower than the design value of 2.00 mm. However, the slot width, t_s , was observed to have dimensions between 1.24 mm and 1.25 mm compared to its design value of 1.20 mm.

The S45C-02 shaft mover exhibits larger and more inconsistent dimensional deviations than other shaft movers. Some point positions might be closer to the design value, whereas others might not be. The tooth width, t_w , was manufactured within the range of 0.73–0.78 mm, which is slightly smaller than the designed value 0.80 mm. Meanwhile, the slot width, t_s , had a value in the range of 1.22 mm to 1.28 mm compared to 1.20 mm as its design value. In the case of tooth pitch, τ_p , some points of position are located higher than their design value, whereas some other positions are the opposite. The range of deviation was between 1.96 and 2.04 mm compared to its design value of 2.00 mm.

To evaluate the effect of manufacturing tolerance, Δx , consistency, on the SRLSM shaft mover dimensions, the accumulated tooth dimensions of the manufactured samples were compared with the corresponding design values. The SRLSM shaft

mover dimensions were measured based on a specific measuring point, n_{mp} . Fig. 9 shows the sequence of measuring points, n_{mp} , for the S45C-01 and S45C-02 shaft movers. The sequence of measuring points, n_{mp} , of 1 was considered the origin point (0 mm). The dimension of the subsequent measuring point, n_{mp} , is represented by the distance between the instantaneous measuring point, n_{mp} , and its origin. Because the S45C-02 shaft mover was manufactured to be longer than the S45C-01, the numbering for the measuring point, n_{mp} , for the S45C-02 shaft mover was higher than that for the S45C-01 shaft mover.

Figure 10 shows the accumulated dimension and tolerance of the shaft mover of the SRLSM. Due to the constant manufacturing tolerance, Δx , on each element in the S45C-01 shaft mover, the accumulated tolerance, Δx_{total} , increases as the sequence of the measuring point, n_{mp} , increases. Thus, the difference between the designed and manufactured accumulated dimensions d_{total} also becomes significant at higher sequences of the measuring point, n_{mp} . Assuming that the stator of the SRLSM was manufactured with zero tolerance, the teeth of the mover shaft are likely to be shifted compared with the stator teeth of the SRLSM, which could influence the thrust. Based on Fig. 10(a), the total accumulated tolerance, Δx_{total} , for the S45C-01 mover shaft at the last measuring point, n_{mp} , is ap-

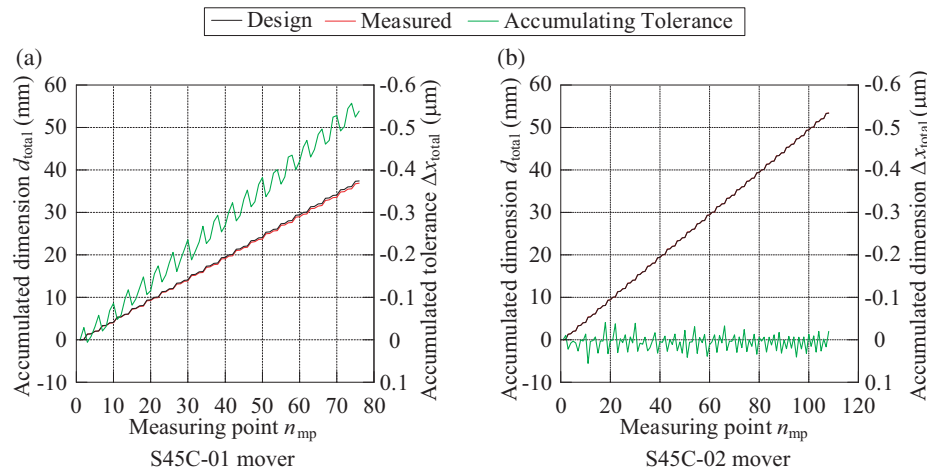


FIGURE 10. Accumulated dimension and tolerance of the SRLSM's movers.

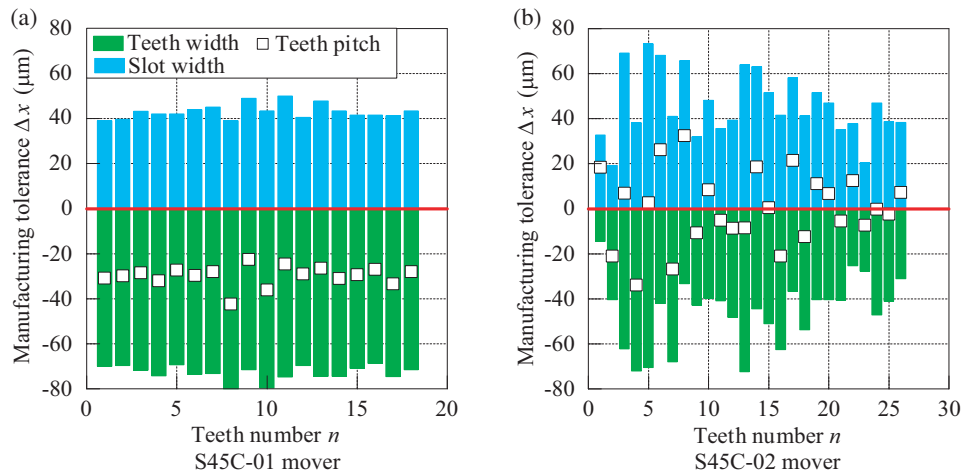


FIGURE 11. Manufacturing tolerance, Δx , estimation based on measured dimension of the SRLSM's mover.

proximately $-562.3 \mu\text{m}$. It means that the mover shaft was manufactured smaller than the design value. Compared to the design value of 37.4 mm , this shaft mover has a dimension of 36.84 mm at the final measuring point, n_{mp} .

Unlike for the S45C-02 shaft mover as shown in Fig. 10(b), owing to the inconsistency of the manufacturing tolerance, Δx , the accumulated tolerance, Δx_{total} , is lower and almost close to $0 \mu\text{m}$ compared with the S45C-01 shaft mover. The manufacturing tolerance, Δx , value of the previous teeth could reduce the manufacturing tolerance, Δx , of the subsequent teeth, thus making the accumulated tolerance, Δx_{total} , become small. Therefore, the difference between the designed and measured accumulated dimensions d_{total} also becomes insignificant regardless of the sequence of the measuring point, n_{mp} . The shift of the shaft mover teeth compared to the 0 tolerance of the stator teeth can be minimized. Thus, the influence of the thrust is reduced. At the final measuring point, n_{mp} , the design dimension was 53.4 mm compared to the measured value of 53.38 mm . The shaft mover was manufactured smaller than the design value with an accumulated tolerance, Δx_{total} , of $-20 \mu\text{m}$, which was smaller than the S45C-01 shaft mover.

Based on Figs. 8 and 10, the manufacturing tolerance, Δx , for the tooth width, t_w , slot width, t_s , and tooth pitch, τ_p , at each tooth number as shown in Fig. 6, were calculated. The results are shown in Fig. 11. For the S45C-01 shaft mover, as shown in Fig. 11(a), the tooth width, t_w , and tooth pitch, τ_p , were smaller than their design values. It can be confirmed with the negative value of the manufacturing tolerance, Δx . The range of the manufacturing tolerance, Δx , for both elements are $-68.6 \mu\text{m}$ to $-81.5 \mu\text{m}$ and $-22.6 \mu\text{m}$ to $-42.4 \mu\text{m}$, respectively. Opposite characteristics have been found for the slot width, t_s , where it was manufactured larger than its design value, thus the positive value of the manufacturing tolerance, Δx , was observed in the range of $39.1 \mu\text{m}$ to $50.1 \mu\text{m}$.

For the S45C-02 shaft mover, as shown in Fig. 11(b), the manufacturing tolerance, Δx , for the tooth width, t_w , and slot width, t_s , shows a similar pattern to the S45C-01 shaft mover. The tooth width, t_w , was manufactured smaller than the design value with manufacturing tolerance, Δx , in the range of $-14.5 \mu\text{m}$ to $-72.4 \mu\text{m}$, and the slot width, t_s , was manufactured larger than the design value with the manufacturing tolerance, Δx , in the range of $19.2 \mu\text{m}$ to $73.2 \mu\text{m}$. Meanwhile, the manufacturing tolerance, Δx , for the tooth pitch, τ_p , exhibited

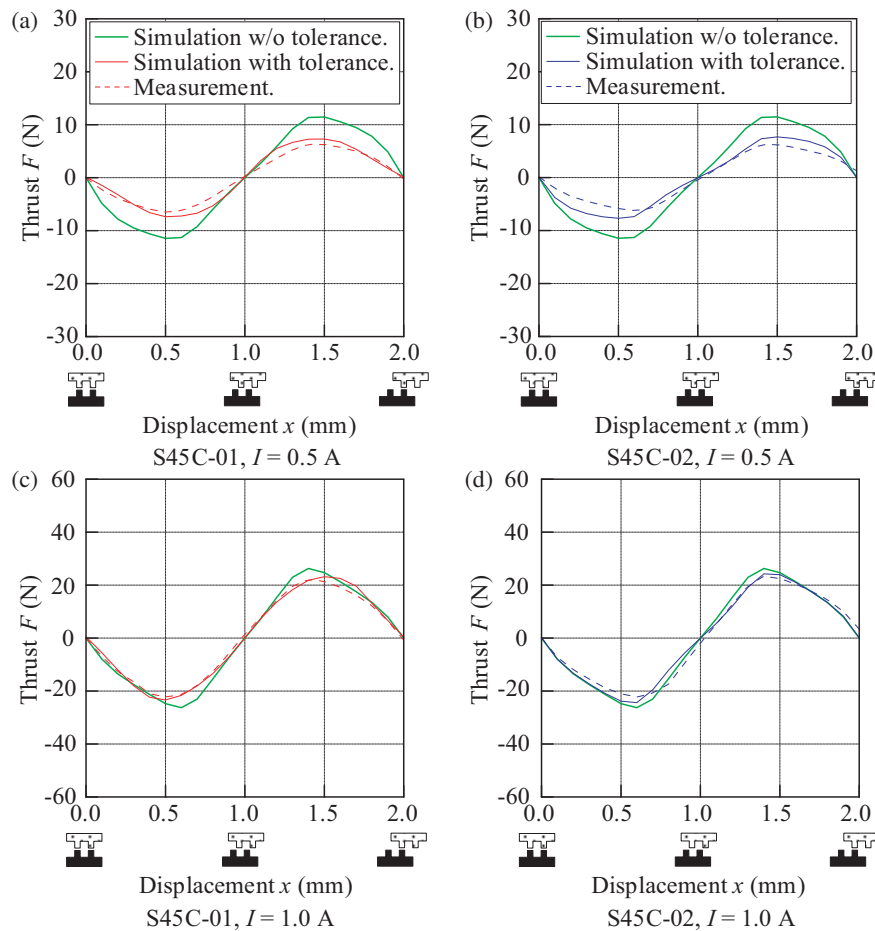


FIGURE 12. Comparison of thrust characteristics.

a fluctuating pattern. At some points, the manufacturing tolerance, Δx , is a positive value, while at others, it has negative value. The range of manufacturing tolerance, Δx , is between $32.5 \mu\text{m}$ and $-33.9 \mu\text{m}$.

Dimensional analysis of shafts S45C-01 and S45C-02 highlighted significant differences in both the mean values and variability across key components, namely the tooth width, slot width, and tooth pitch. For S45C-01, the standard deviation values were relatively low, ranging from 3.18 to 4.42, indicating high manufacturing consistency. Among its components, the slot width shows the smallest variation, while the tooth pitch exhibits the highest. The mean values for tooth width and tooth pitch were negative, suggesting a directional offset, whereas the slot width remained positive. In contrast, S45C-02 demonstrated considerably higher variability, with standard deviation values between 14.56 and 16.33. Although the mean teeth pitch was close to zero, its large standard deviation indicated poor dimensional stability. The tooth width and slot width also showed substantial deviations, reflecting less control over the manufacturing accuracy.

Comparing the same components across the shafts, S45C-01 was far more stable than S45C-02 for all dimensions. For example, the tooth width in S45C-01 has a standard deviation of 3.47 compared to 14.91 in S45C-02, while the slot width shows similar mean values for both shafts but much lower variability in S45C-01. The most striking difference was observed in

tooth pitch, where S45C-01 has a large negative mean, whereas S45C-02 is nearly zero, though with high variability. Overall, S45C-01 demonstrated better dimensional stability, which is advantageous for quality control and long-term reliability. Conversely, S45C-02, despite its higher variability, may offer better alignment with design specifications for certain critical dimensions, potentially influencing performance outcomes, such as force generation.

4.2. Evaluation of Thrust Characteristics of the SRLSM under Different Shaft Movers

The thrust characteristics of the SRLSM under all conditions are shown in Fig. 12. Despite having similar patterns, at lower currents, the difference between the simulation outputs without and with tolerance cases is significant for both shafts. However, the differences become insignificant at higher currents because the saturation effect begins to occur. The thrust characteristics between the simulation and measurement under the influence of manufacturing tolerances are not significant.

Figure 13 compares the maximum thrust values of the SRLSM under different operating conditions and illustrates the corresponding variations in thrust characteristics. There are three classifications of thrust observed in this study. The definition for each classification is as follows:

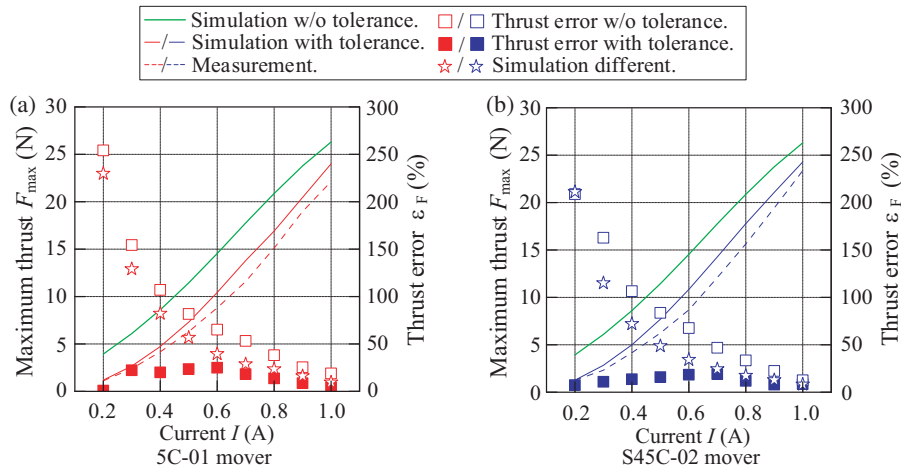


FIGURE 13. Comparison of maximum thrust, F_{max} , and thrust error, ϵ_F , of the SRLSM with different types of movers.

- a. Simulation difference: -difference between simulated thrusts with and without manufacturing tolerance.
- b. Thrust error without tolerance: -difference between simulated thrusts without manufacturing tolerance and measured thrust.
- c. Thrust error with tolerance: -difference between simulated and measured thrusts with manufacturing tolerance.

Based on the figure, the effect of manufacturing tolerance results in a significant difference between the simulation outputs. The percentage error is high at low currents and decreases as the current increases. This is because of the possibility of a saturation effect occurring in the SRLSM structure. For the S45C-01 shaft, the highest percentage error is found equal to 230% at a current of 0.2 A and 9.6% at a current of 1.0 A. For the S45C-02 shaft, the highest percentage error is found equal to 211% at a current of 0.2 A and 8.3% at a current of 1.0 A. It is shown that the manufacturing tolerance, Δx , had the potential to reduce the thrust characteristics compared to the zero manufacturing tolerance, Δx , model.

The thrust error between the measured thrust and simulation output under zero manufacturing tolerance was also investigated. A similar pattern was observed in this comparison. For the S45C-01 shaft, the highest percentage error was 254%, and for the S45C-02 shaft, the highest percentage error at the current was 208%. The lowest percentages were 18.8% and 12.6% for 1 A currents S45C-01 and S45C-02 shafts, respectively. The lower error observed in the S45C-02 shaft is attributed to its smaller accumulated manufacturing tolerance, Δx_{total} , than that of the S45C-01 shaft.

The thrust error between the simulated and measured outputs, taking into account the manufacturing tolerance for each shaft, was analyzed. The thrust patterns for the two outputs were in good agreement. Furthermore, the thrust error values were reduced compared to those in the earlier cases. It shows that the simulation model and fabricated prototype have similar conditions. The thrust error values were reduced from 230% and 254% to 7.4% for the S45C-01 shaft at 0.2 A and from 9.6% and 18.8% to 8.4% at 1.0 A. For the S45C-02 shaft, the thrust error

was reduced from 211% and 208% to 8% and from 8.3% and 12.6% to 4% at current of 0.2 A and 1.0 A, respectively. By incorporating the manufacturing tolerance, Δx , into the simulation, the thrust error between simulated and measured results for both S45C-01 and S45C-02 shafts was significantly reduced. This demonstrates good agreement between the simulated model and fabricated prototype across different current values.

To further estimate the effect of the manufacturing tolerance, Δx , on the thrust of the SRLSM, the thrust sensitivity, S_F , is calculated for each excitation current, as shown in Fig. 14. The thrust sensitivity, S_F , was calculated using Equation (6). Based on Fig. 14, it is shown that the measured thrust value is more influenced by the manufacturing tolerance, Δx , than the simulated thrust. Furthermore, it is observed that the sensitivity is higher at low current excitation, indicating that the system is more vulnerable to dimensional variation under unsaturated conditions.

$$S_F = \frac{|F_{S45C-01} - F_{S45C-02}|}{\Delta x_{S45c-01} \Delta x_{S45c-02}} \quad (6)$$

where S_F is the thrust sensitivity of the SRLSM in (F/m); $F_{S45C-01}$ and $F_{S45C-02}$ are the thrusts of the SRLSM with S45C-01 and S45C-02, respectively, in (N); and $\Delta x_{S45C-01}$ and $\Delta x_{S45C-02}$ are manufacturing tolerances of the S45C-01 and S45C-02, respectively, in (m).

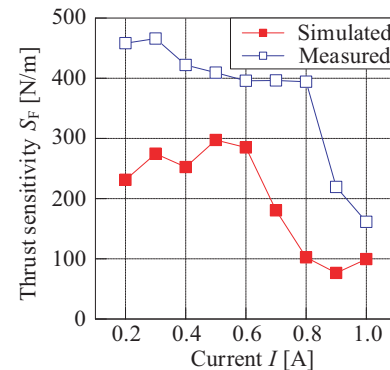


FIGURE 14. Thrust sensitivity of the SRLSM.

5. CONCLUSION

The effect of manufacturing tolerance, Δx , on the SRLSM thrust for two sets of SRLSM movers is investigated, with different accumulated manufacturing tolerances, Δx_{total} . The S45C-01 shaft has an accumulated manufacturing tolerance, Δx_{total} , of $-562.3 \mu\text{m}$ while the S45C-02 shaft has a lower accumulated manufacturing tolerance, Δx_{total} , which is $-20 \mu\text{m}$. Then, the thrust characteristics were acquired through simulation and measurement outputs. The measurements were conducted using both shafts, while the simulations were executed based on zero and actual manufacturing tolerance, Δx , value for each shaft. The thrust characteristics based on all conditions and methods have been compared. As a result, the manufacturing tolerance, Δx , leads to a significant increase in the thrust error, defined as the difference between the simulated and measured outputs. To reduce thrust error, the simulation model needs to be set with the same manufacturing tolerance, Δx , as the manufactured prototype. The reduction in thrust is attributed to the decrease in the rate of change of inductance, caused by the misalignment of stator and mover teeth due to dimensional deviations. Furthermore, the results indicate that thrust degradation is strongly correlated with accumulated manufacturing tolerance. This statement was proven by the result of thrust sensitivity, S_F , where the machine with a larger tolerance exhibits significantly higher deviation from the ideal case. It should be noted that stator manufacturing tolerances are not explicitly measured in this study due to limitations of the Vision Measurement System, which is primarily configured for mover inspection. Nevertheless, since the stator and mover were fabricated using similar manufacturing processes, it is reasonable to assume that the resulting tolerances are comparable. Therefore, the total observed tolerance effect can be approximated as a combined contribution from both components, where the measured variation is assumed to be equally influenced by the mover and stator.

ACKNOWLEDGEMENT

The authors would like to thank Universiti Teknikal Malaysia Melaka (UTeM) for providing funding for this research.

REFERENCES

- [1] Li, L., J. Zhang, S. Qiu, H. Huang, W. Yan, and C. Zhang, "Analysis of structural tolerance influences on thrust ripple of U-shaped ironless permanent magnet linear motor," in *IECON 2023- 49th Annual Conference of the IEEE Industrial Electronics Society*, 1–6, Singapore, 2023.
- [2] Boscaino, V., G. Cipriani, V. D. Dio, M. Corpora, D. Curto, V. Franzitta, and M. Trapanese, "Experimental validation of a distribution theory based analysis of the effect of manufacturing tolerances on permanent magnet synchronous machines," *AIP Advances*, Vol. 7, No. 5, 056650, 2017.
- [3] Dinh, B. M. and D. H. Linh, "Torque performances of switched reluctance motor 12/8 by rotor pole embrace verification," in *Proceedings of the 11th Annual International Conference on Industrial Engineering and Operations Management*, 4340–4351, Singapore, 2021.
- [4] García-Amorós, J., P. Andrada, and B. Blanqué, "Assessment of linear switched reluctance motor's design parameters for optimal performance," *Electric Power Components and Systems*, Vol. 43, No. 7, 810–819, 2015.
- [5] Emarloo, A. A., L. Papini, and P. Bolognesi, "Extended-speed-range low-torque-ripple control for unsaturated switched reluctance motors," in *2025 IEEE Workshop on Electrical Machines Design, Control and Diagnosis (WEMDCD)*, 1–7, Valletta, Malta, 2025.
- [6] Saadha, A., C. V. Aravind, P. Krishna, and F. Azhar, "Analysis of taper width variations in linear reluctance machine," *Journal of Engineering Science and Technology*, Vol. 13, 17–26, 2018.
- [7] Hirayama, T., Y. Nakamori, T. Yamada, and S. Kawabata, "Experimental characterization of linear switched reluctance motor for physical distribution conveyance system," in *2018 21st International Conference on Electrical Machines and Systems (ICEMS)*, 1832–1835, Jeju, Korea (South), 2018.
- [8] Sial, M. R. and N. C. Sahoo, "Online phase excitation angle control for four quadrant operation of switched reluctance motor drive," *Journal of Control and Decision*, 1–19, 2025.
- [9] Abdulah, N., F. A. A. Shukor, R. Othman, S. Ahmad, and N. Nasir, "Modelling methods and structure topology of the switched reluctance synchronous motor type machine: A review," *International Journal of Power Electronics and Drive Systems (IJPEDS)*, Vol. 14, No. 1, 111–122, 2023.
- [10] Castano, S. M., M. A. Montilla, and J. Maixé-Altés, "Acoustic noise in a Switched Reluctance Motor drive: Torque-speed control and effect of failure," in *2013 Workshop on Power Electronics and Power Quality Applications (PEPQA)*, 1–6, Bogota, Colombia, 2013.
- [11] Nitabaru, T., H. Okada, T. Isomura, Y. Kawashima, H. Abe, and H. Ogata, "Drive control development of switched reluctance motor for compact electric vehicles," *SAE International Journal of Advances and Current Practices in Mobility*, Vol. 1, No. 3, 1006–1013, 2019.
- [12] Madonna, V., C. M. Meano, and K. F. Hansen, "Performance improvement of switched reluctance machines through appropriate design choices," in *2025 IEEE Workshop on Electrical Machines Design, Control and Diagnosis (WEMDCD)*, 1–7, Valletta, Malta, 2025.
- [13] Chen, H., J. Liu, X. Li, M. Orabi, and Y. Li, "Switched reluctance linear motor force ripple suppression based on predictive-fuzzy control," in *2021 13th International Symposium on Linear Drives for Industry Applications (LDIA)*, 1–9, Wuhan, China, 2021.
- [14] Pan, J. F., N. C. Cheung, and Y. Zou, "An improved force distribution function for linear switched reluctance motor on force ripple minimization with nonlinear inductance modeling," *IEEE Transactions on Magnetics*, Vol. 48, No. 11, 3064–3067, Nov. 2012.
- [15] Kim, T., M. Chowdhury, M. Islam, A. Gebregergis, and T. Sebastian, "Tolerance study to forecast performances of permanent magnet synchronous machines using segmented stator for mass production," *IEEE Transactions on Industry Applications*, Vol. 54, No. 5, 4333–4342, Sep.–Oct. 2018.
- [16] Ershad, N. F., W. Jensen, J. Kim, M. Muir, E. Kaiser, and A. Ramm, "Manufacturing parameter variation effects on performance and energy loss on ultium traction motors," in *2022 IEEE Energy Conversion Congress and Exposition (ECCE)*, 1–6, Detroit, MI, USA, 2022.
- [17] Li, C., M. Huang, W. Li, N. Wang, and J. Fu, "Optimization of an induction motor for loss reduction considering manufacturing tolerances," *Structural and Multidisciplinary Optimization*,

- Vol. 65, No. 7, 187, 2022.
- [18] Müller, C., M. Franck, M. Schröder, M. Balluff, A. Wanke, and K. Hameyer, "Impact study of isolated and correlated manufacturing tolerances of a permanent magnet synchronous machine for traction drives," in *2019 IEEE International Electric Machines & Drives Conference (IEMDC)*, 982–987, San Diego, CA, USA, 2019.
- [19] Amoros, J. G. and G. P. Andrada, "Magnetic circuit analysis of a linear switched reluctance motor," in *2009 13th European Conference on Power Electronics and Applications*, 1–9, Barcelona, Spain, 2009.
- [20] Somesan, L.-E., E. Padurariu, and I.-A. Viorel, "Two simple analytical models, direct and inverse, for switched reluctance motors," *Progress In Electromagnetics Research M*, Vol. 29, 279–291, 2013.
- [21] Nam, T.-H., I.-S. Song, J. Jung, H.-W. Yang, D. Jang, and S.-Y. Jung, "Deep learning-based robust design of a CNC servo motor considering manufacturing tolerances," in *2025 28th International Conference on Electrical Machines and Systems (ICEMS)*, 1–6, Busan, Korea, 2025.
- [22] Chen, S., Y. Liu, Q. Zhang, and J. Tan, "Analysis and suppression of thrust ripple in a permanent magnet linear synchronous motor — A review," *Energies*, Vol. 18, No. 4, 863, 2025.